

To appear on the Proceedings of the 13th ICATPP Conference on
Astroparticle, Particle, Space Physics and Detectors
for Physics Applications,
Villa Olmo (Como, Italy), 3–7 October, 2011,
to be published by World Scientific (Singapore).

HELIOSPHERE DIMENSION AND COSMIC RAY MODULATION

P. Bobik¹, M.J. Boschini^{2,4}, C. Consolandi², S. Della Torre^{2,5}, M. Gervasi^{2,3,*}, D.
Grandi², K. Kudela¹, F. Noventa^{2,3}, S. Pensotti^{2,3}, P.G. Rancoita², D. Rozza^{2,3}

¹ *Institute of Experimental Physics, Kosice (Slovak Republic)*

² *Istituto Nazionale di Fisica Nucleare, INFN Milano-Bicocca, Milano (Italy)*

³ *Department of Physics, University of Milano Bicocca, Milano (Italy)*

⁴ *CILEA, Segrate (MI) (Italy)*

⁵ *Department of Physics and Maths, University of Insubria, Como (Italy)*

**E-mail: massimo.gervasi@mib.infn.it*

The differential intensities of Cosmic Rays at Earth were calculated using a 2D stochastic Montecarlo diffusion code and compared with observation data. We evaluated the effect of stretched and compressed heliospheres on the Cosmic Ray intensities at the Earth. This was studied introducing a dependence of the diffusion parameter on the heliospherical size. Then, we found that the optimum value of the heliospherical radius better accounting for experimental data. We also found that the obtained values depends on solar activity. Our results are compatible with Voyager observations and with models of heliospherical size modulation.

Keywords: Cosmic rays; Solar Modulation; Monte Carlo simulations

1. The 2D Model of the Heliosphere

HelMod Code¹ solves the bi-dimensional Parker's particle transport equation². A Monte Carlo technique is applied on a set of Stochastic Differential Equations (SDEs) fully equivalent to the Parker's equation³. The model takes into account particle drift effects and latitudinal dependence of the solar wind speed and of the Interplanetary Magnetic Field (IMF). It is described in details in Ref. 1. In the model, the IMF from Parker⁴ is modified introducing a small latitudinal components as described in Ref. 5. For periods of low solar activity, we take a solar wind speed gradually increasing from the Earth position up to a maximum value near the heliospherical poles ($\simeq 760$ km/s)⁶. For periods approaching the solar maximum we as-

sume a solar wind speed independent on the latitude.

The symmetric part of the diffusion tensor, in a reference frame with one axis aligned with the Parker's magnetic-field, is purely diagonal containing transverse ($K_{\perp\theta}$ and $K_{\perp r}$) and parallel (K_{\parallel}) components⁷. The diffusion coefficients are given by⁸

$$\begin{aligned} K_{\parallel} &= \beta K_0(t) K_P(P) \left[\frac{B_{\oplus}}{3B} \right], \\ K_{\perp r} &= \rho_k K_{\parallel}, \\ K_{\perp\theta} &= \iota(\theta) \rho_k K_{\parallel}, \end{aligned} \quad (1)$$

where $\beta = v/c$, v the particle velocity and c the speed of light; the diffusion parameter K_0 accounts for the dependence on the solar activity; B_{\oplus} is the measured value of IMF at the Earth position - typically ≈ 5 nT, but changing with time - obtained from Ref. 9; B is the magnitude of the large scale IMF as a function of heliocentric coordinates; finally, the term K_P takes into account the dependence on the rigidity P of the GCR particle usually expressed in GV. In the present model $K_P \approx P$ (e.g., see Ref.¹⁰). Furthermore $\rho_k = 0.05$ and, as described in Ref. 1,

$$\iota(\theta) = \begin{cases} 10, & \text{in the polar regions,} \\ 1, & \text{in the equatorial region.} \end{cases} \quad (2)$$

After the transformations from 3D field-aligned into 2D heliospherical coordinates¹¹, the symmetric components of the diffusion tensor contains both diagonal (K_{rr} and $K_{\theta\theta}$) and off-diagonal terms ($K_{r\theta}$ and $K_{\theta r}$), resulting by a proper combination of $K_{\perp\theta}$, $K_{\perp r}$ and K_{\parallel} ¹.

2. The Diffusion Parameter

K_0 accounts for the dependence on the solar activity. We estimated K_0 by using the modulation strength ϕ_s , in the framework of the Force Field (FF) approximation¹². ϕ_s was evaluated starting from Neutron Monitor (NM) counting rates in Ref. 13. We moreover used a practical correlation of K_0 with the level of solar activity in the different solar phases¹. We used, as solar activity monitor, the Smoothed Sunspot Number (SSN).

This method is sensitive to the modulation of the GCR flux integrated over the full heliosphere, from the outer boundary to the Earth position, down to a lower limit in rigidity of $\sim (2-3)$ GV. This limit is fixed by the sensitivity of the NM network, due to the geomagnetic rigidity cut-off and to the atmospheric yield function. The outer boundary of the heliosphere

is located at the position of the Termination Shock. Beyond this limit the model of heliosphere we are using is not more valid. Moreover, the additional modulation occurring in the heliosheat only affects particles with rigidity well below 1 GV^{14,15}. The method is sensitive also to the LIS used for the estimation of the modulation strength, but several LIS spectra do not differ each other above this rigidity limit. Finally the diffusion parameter depends on the outer boundary position, as follows from the FF approximation:

$$K_0(t) = \frac{V_{sw}(t)(R_{TS} - R_{earth})}{3\phi_s(t)}. \quad (3)$$

In Ref. 1 the boundary of heliosphere was placed at 100 AU. The solar cavity was split in 15 spherical regions to take into account the time spent by SW to travel outward. In each region of the interplanetary space, the parameters (i.e., SW speed, SSN, B_{\oplus} , tilt angle) are related to the solar activity at the time of the injection of the solar wind diffusing in that region¹⁶. In this way modulated intensities of protons, down to ~ 400 MeV, were simulated and successfully compared with experimental data covering roughly one solar cycle. We did not find significant differences changing the position of the outer boundary of the heliosphere¹.

3. Heliospherical Size and Diffusion Parameter

In the past years the position of the Termination Shock was estimated through the observations of Voyager 1 and Voyager 2 spacecrafts (see Refs. 17,18 and Table 1). In addition several authors (see Refs. 19,20) suggest that the size of the heliosphere should change with the solar activity, following a quasi-periodic feature, roughly anti-correlated with the SSN.

Table 1. Voyager crossings of Termination Shock.

	R_{TS} (AU)	solar latitude (deg)
Voyager 1	94.0	+ 34.3
Voyager 2	83.7	- 27.5

Following these results we evaluated the effect of stretched and compressed heliospheres on the Cosmic Ray intensities at the Earth introducing a dependence of the diffusion parameter on the heliospherical size. We defined a new diffusion parameter K_0^* , introducing the parameter $r(R_{TS}, P)$ sensitive to the position of the Termination Shock:

$$K_0^*(R_{TS}) = r(R_{TS}, P) K_0(100 \text{ AU}) \quad (4)$$

$$r(R_{TS}, P) = 1 + f(P) \left[\frac{R_{TS}(\text{AU}) - 100}{99} \right]. \quad (5)$$

$r(R_{TS}, P)$ allows to modify the value of the diffusion parameter adapting it to a different volume of the heliosphere, determined by R_{TS} . $r(R_{TS}, P)$ is fully effective below a rigidity limit P_1 . We also defined a transition function $f(P)$:

$$f(P) = \begin{cases} 0, & \text{for } P \geq P_2, \\ (P_2 - P)/(P_2 - P_1), & \text{for } P_1 < P < P_2, \\ 1, & \text{for } P \leq P_1. \end{cases} \quad (6)$$

For rigidity higher than P_2 , the dependence on R_{TS} can be neglected. Here the diffusion parameter is still defined for an heliospherical dimension of 100 AU. The dependence on the heliospherical radius R_{TS} is then effective at rigidity lower than P_2 . Using the novel diffusion parameter $K_0^*(R_{TS}, P)$ we simulated the modulated spectra, for different values of R_{TS} , P_1 and P_2 , extending the modulated spectra down to a lower rigidity.

4. Results

We compare our simulated spectra with proton data extended down to a kinetic energy of 200 MeV. Here we present results obtained using the following rigidity parameters: $P_2 = P_1 = 1.0$ GV. We used the Local Interstellar Spectrum (LIS) from Ref. 21 and compared it with the LIS from GALPROP²². In Fig. 1 the results compared with AMS-01 data²³ are shown, assuming $R_{TS} = 120$ AU, as discussed later on.

We estimated the best value of R_{TS} , looking at the RMS differences (η_{RMS}) with experimental data:

$$\eta_{\text{RMS}} = \sqrt{\frac{\sum_i (\eta_i / \sigma_{\eta,i})^2}{\sum_i 1 / \sigma_{\eta,i}^2}}, \quad (7)$$

with

$$\eta_i = \frac{f_{\text{sim}}(T_i) - f_{\text{exp}}(T_i)}{f_{\text{exp}}(T_i)}, \quad (8)$$

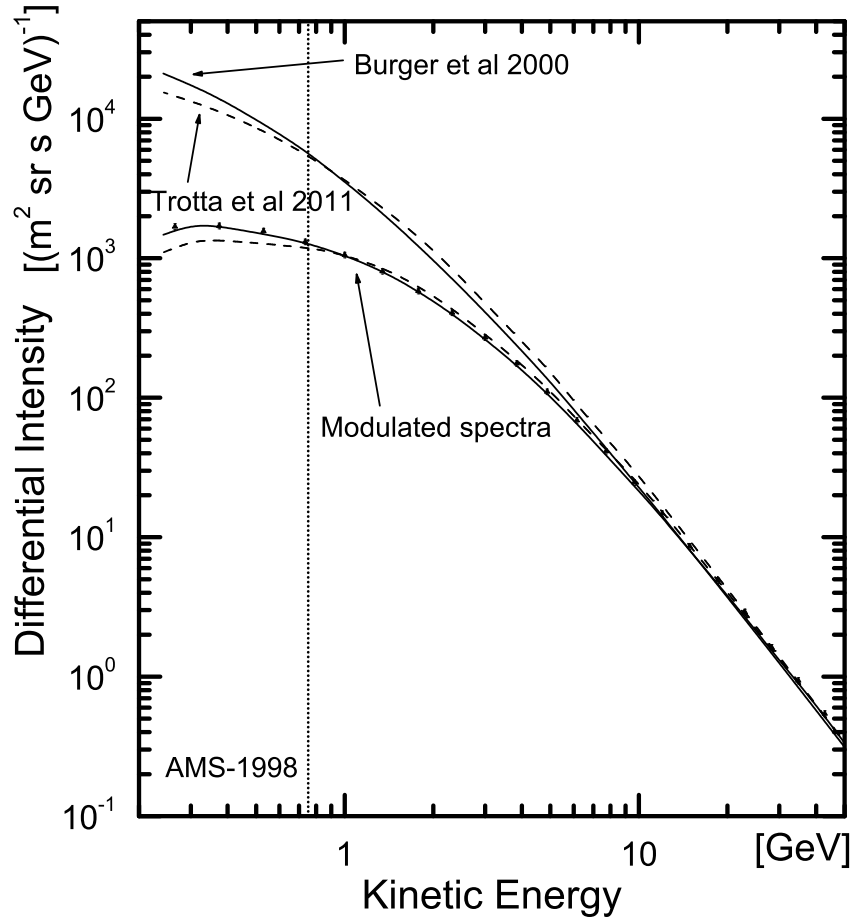


Fig. 1. Modulated proton spectra and comparison with AMS-01 data²³. LIS are taken from Ref. 21 and GALPROP²². The vertical dotted line represents the lower limit of the sensitivity of the NM. Above this limit the two LIS are not significantly different.

where T_i is the average energy of the i -th energy bin of the differential intensity distribution and $\sigma_{\eta,i}$ are the error bars including the experimental and Monte Carlo uncertainties. For each experimental spectrum we got the best values of R_{TS} shown in Table 2 together with the minimum value of η_{RMS} . Data from BESS flights are given in Ref. 24, data from AMS-01 are given in Ref. 23.

In Fig. 2 modulated spectra, obtained using values of R_{TS} reported in Table 2, are shown in comparison with BESS experimental data. Modulated

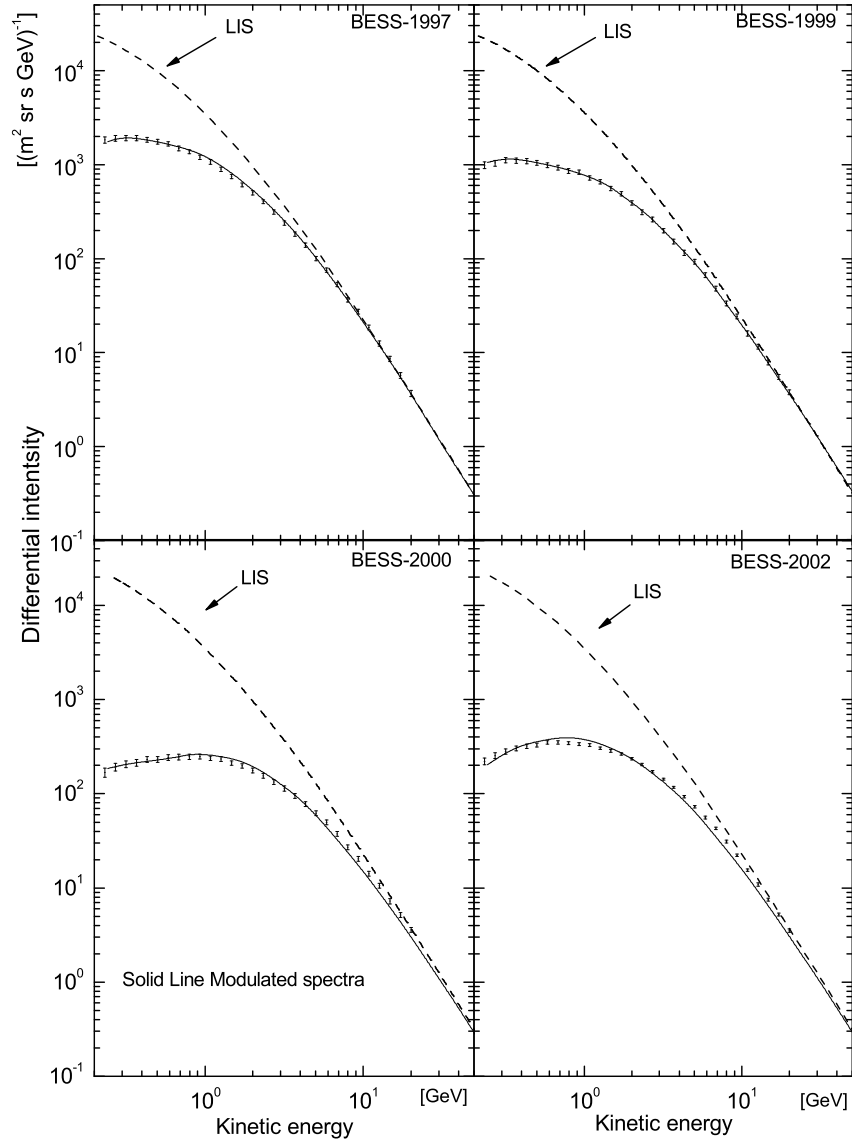


Fig. 2. Modulated proton spectra and comparison with BESS-1997, BESS-1999, BESS-2000, BESS-2002 observing data²⁴.

spectrum compared with AMS-01 data has been shown in Fig. 1. We did not use data measured by Pamela²⁵ because published spectra start from

Table 2. Best values of R_{TS} , its minimum and maximum values, and RMS differences between simulations and experimental data.

	R_{TS}^{best} (AU)	R_{TS}^{min} (AU)	R_{TS}^{max} (AU)	η_{RMS} (%)
BESS-1997	115	100	130	7.05
AMS-1998	120	110	135	4.86
BESS-1999	120	110	130	3.35
BESS-2000	140	125	150	10.00
BESS-2002	105	95	115	11.78

400 MeV, while our analysis is more sensitive below this limit. In Table 2 we report the interval of values of R_{TS} where η_{RMS} does not change by more than $\sim (2 - 3)$ % from its minimum value, reported in the last column. This variation roughly represents the uncertainty of the computation itself, and it is determined comparing simulations and data at energies larger than (10 – 20) GeV, i.e. above the region of solar modulation. Results are shown in Fig. 3 in comparison with models²⁰ and Voyager measurements^{17,18}.

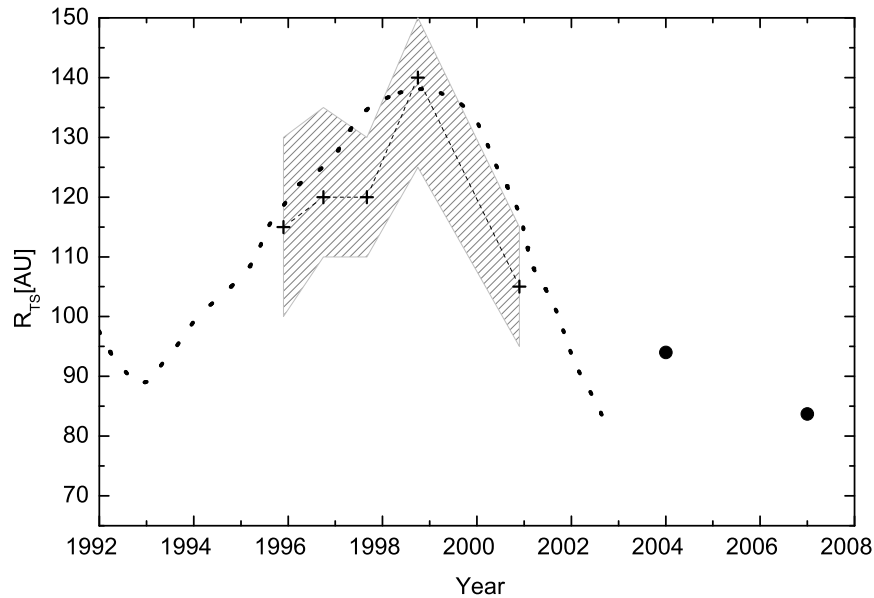


Fig. 3. R_{TS} best value for the several experiments (crosses) in comparison with Voyager data^{17,18} (dots) and models²⁰ (dashed line). The shadow represents the region between the minimum and maximum value, as reported in Table 2.

As shown in Fig. 1 and Fig. 2, modulated spectra succeed to fit observing data, in particular during periods of low solar activity. For more accurate results we need more accurate experimental data. Current error bars are of the order of 5% or even larger. Moreover systematic deviations are present looking at different data sets at energy above (20–30) GV, where spectra are not affected by solar modulation. In addition current observation data, taken on board of stratospheric balloons or space orbiters, may be contaminated at low energy by secondaries produced inside the Earth magnetosphere. A LIS spectrum with a slightly different shape could be also preferred to fit better low energy data. Finally a refinement of our model could be requested, starting with a slightly different values of P_2 and P_1 , in order to smooth the ripple present in some spectrum. In the future a model with an aspheric Heliosphere can be also developed.

5. Conclusions

We presented the HelMod 2D Monte Carlo code for the study of Cosmic Rays propagation in the inner heliosphere. Both heliospherical shape and size are supposed to be relevant for the modulation process. We introduced a dependence of the diffusion parameter on the heliospherical size, which accounts for the variation with time and solar activity. We compare modulated spectra with experimental data covering the solar cycle 23. Then we found, for our 2D model, the best value of the heliospherical radius, which changes with time. Most of the solar modulation occurs in the inner heliosphere and differences in the heliospherical radius are effective only at energy below a few hundred MeV. Our results are not in contradiction with Voyager observations and models of TS distance as a function of solar activity. We found that LIS from Ref. 21 fits better observation data at low energy.

Acknowledgments

Authors acknowledge the use of NASA/GSFCs Space Physics Data Facilitys OMNIWeb service, and OMNI data.

References

1. P. Bobik, G. Boella, M.J. Boschini, C. Consolandi, S. D. Torre, M. Gervasi, D. Grandi, K. Kudela, S. Pensotti, P.G. Rancoita, M. Tacconi, *Astrophys. J.*, in press, (2011); arXiv:1110.4315 [astro-ph.SR] 19 Oct 2011.
2. E. N. Parker, *Plan. & Space Sci.* **13**, p. 9 (1965).

3. P. Bobik, M. Boschini, C. Consolandi, S. Della Torre, M. Gervasi, D. Grandi, K. Kudela, S. Pensotti and P.G. Rancoita, *Astrophys. Space Sci. Trans.* **7**, 245 (2011).
4. E. N. Parker, *Astrophys. J.* **128**, 664 (1958).
5. U. Langner, *Ph.D. Thesis, Potchestroom University* (2004).
6. D. J. McComas, B. L. Barraclough, H. O. Funsten, J. T. Gosling, E. Santiago-Muñoz, R. M. Skoug, B. E. Goldstein, M. Neugebauer, P. Riley and A. Balogh, *J. Geophys. Res.* **105**, 10419 (2000).
7. M. S. Potgieter, *J. Geophys. Res.* **105**, 18295 (2000).
8. M. S. Potgieter and J. A. Le Roux, *Astrophys. J.* **423**, p. 817 (1994).
9. Omniweb data available at: <http://omniweb.gsfc.nasa.gov/form/dx1.html> (2011).
10. J. S. Perko, *Astron. and Astrophys.* **184**, 119 (1987).
11. R. A. Burger, T. P. J. Krüger, M. Hitge and N. E. Engelbrecht, *Astrophys. J.* **674**, 511 (2008).
12. L. J. Gleeson and W. I. Axford, *Astrophys. J. Lett.* **149**, L115 (1967).
13. I.G. Usoskin, et al., *J. Geophys. Res.* **110**, A12108 (2005).
14. Bobik, P., K. Kudela, M. Boschini, D. Grandi, M. Gervasi, P.G. Rancoita, Solar modulation model with reentrant particles, *Adv. Space Res.*, **41** (2008), 339-342, doi:10.1016/j.asr.2007.02.085.13.
15. Scherer, K., Fichtner, H., Strauss, R. D., et al., *Astrophys. J.*, **735**, 128 (2011), doi:10.1088/0004-637X/735/2/128.
16. P. Bobik, M. Boschini, C. Consolandi, S. Della Torre, M. Gervasi, D. Grandi, K. Kudela, S. Pensotti and P.G. Rancoita, Proton and antiproton modulation in the heliosphere for different solar conditions and AMS-02 measurements prediction, in *Astroparticle, Particle and Space Physics, Radiation Interaction, Detectors and Medical Physics Applications - vol. 6 - Proc. of the 12th ICATPP Conference on Cosmic Rays for Particle and Astroparticle Physics*, 360-368 (2011), eds. S. Giani, C. Leroy, P.-G. Rancoita, ISBN-13 978-981-4329-02-6.
17. E.C. Stone, A.C. Cummings, F.B. McDonald, B.C. Heikkila, N. Lal and W.R. Webber, *Science* **309**, 2017 (2005).
18. E.C. Stone, A.C. Cummings, F.B. McDonald, B.C. Heikkila, N. Lal and W.R. Webber, *Nature* **454**, 71 (2008).
19. Y.C. Whang, L.F. Burlaga, *Geophys. Res. Lett.* **27**, 1607.
20. Y.C. Whang, L.F. Burlaga, Y.-M. Wang, and N.R. Sheeley Jr., *Geophys. Res. Lett.* **31**, L03805 (2004), doi:10.1029/2003GL018679.
21. R. A. Burger, M. S. Potgieter and B. Heber, *J. Geophys. Res.* **105**, 27447 (2000).
22. R. Trotta, G. Johannesson, I.V. Moskalenko, T.A. Porter, R. Ruiz de Austri, and A.W. Strong, *Astrophys. J.* **729**, 106 (2011), doi:10.1088/0004-637X/729/2/106.
23. AMS Collaboration, M. Aguilar *et al.*, *Phys. Rep.* **366**, 331(2002).
24. Y. Shikaze *et al.*, *Astropart. Phys.* **28**, 154 (2007), doi:10.1016/j.astropartphys.2007.05.001.
25. O. Adriani *et al.*, *Science* **332**, 69 (2011), DOI: 10.1126/science.1199172.